Title

Multispectral cross-polarization reflectance measurements suggest high contrast of demineralization on tooth surfaces at wavelengths beyond 1300 nm due to reduced light scattering in sound enamel

Journal

Journal of Biomedical Optics, 23(6)

ISSN

1083-3668

Authors

Chan, Kenneth H
Fried, Daniel

Publication Date

2018-06-01

DOI

10.1117/1.jbo.23.6.060501

Peer reviewed

Journal of Biomedical Optics

BiomedicalOptics.SPIEDigitalLibrary.org

Multispectral cross-polarization reflectance measurements suggest high contrast of demineralization on tooth surfaces at wavelengths beyond 1300 nm due to reduced light scattering in sound enamel

Kenneth H. Chan
Daniel Fried

SPIE.

Kenneth H. Chan, Daniel Fried, "Multispectral cross-polarization reflectance measurements suggest high contrast of demineralization on tooth surfaces at wavelengths beyond 1300 nm due to reduced light scattering in sound enamel," *J. Biomed. Opt.* **23**(6), 060501 (2018), doi: 10.1117/1.JBO.23.6.060501.

Multispectral cross-polarization reflectance measurements suggest high contrast of demineralization on tooth surfaces at wavelengths beyond 1300 nm due to reduced light scattering in sound enamel

Kenneth H. Chan and Daniel Fried*
University of California, San Francisco, Preventive and Restorative Dental Sciences, San Francisco, California, United States

Abstract. The enamel scattering coefficient decreases markedly with increasing wavelength from the visible to the near-infrared (NIR). However, beyond 1300 nm, the scattering coefficient is difficult to measure, and it is not known whether light scattering continues to decrease significantly at longer wavelengths. It is hypothesized that water absorption is a major contributor to the contrast between sound and demineralized enamel beyond 1300 nm since deeply penetrating photons in sound enamel are likely absorbed by water. Reflectance images of demineralization on tooth surfaces were acquired at wavelengths near 1450, 1860, 1880, and 1950 nm. The magnitude of water absorption is similar at 1450 and 1880 nm but varies markedly between 1860, 1880, and 1950 nm. Multispectral comparisons of lesion contrast provide insight into the mechanism responsible for higher contrast at longer NIR wavelengths. The highest contrast was at 1950 nm; however, the markedly higher contrast at 1880 compared to 1450 nm and similar contrast between 1860 and 1880 nm suggests that the enamel scattering coefficient continues to decrease beyond 1300 nm, and that reduced light scattering in sound enamel is most responsible for the higher lesion contrast at longer NIR wavelengths. This has important implications for the choice of wavelengths for caries detection and diagnostic devices, including the performance of optical coherence tomography beyond 1300 nm. [DOI: 10.1117/1.JBO.23.6.060501]

Keywords: dentistry; dental caries; near-infrared reflectance imaging; multispectral imaging; fiber lasers; caries detection.

Paper 180162LRR received Mar. 16, 2018; accepted for publication May 16, 2018; published online Jun. 6, 2018.

The detection and diagnosis of caries lesions (dental decay) is a significant problem in dentistry. Conventional methods rely on a combination of visual and tactile inspection, which are prone to subjective bias, interference from tooth staining, and may incur iatrogenic damage, the latter through the use of a dental explorer.[1] Radiographs have poor sensitivity in diagnosing early occlusal cavities due to overlapping features of the crown. Furthermore, studies have shown that visible- and fluorescence-based caries detection systems suffer false positives from stains.[2–5] A recent summary of caries detection methods is presented by Zandona and Epure.[6] Several studies both *in vitro* and *in vivo* have demonstrated that near-infrared (NIR) reflectance imaging at longer NIR wavelengths (beyond 1300 nm) yields higher contrast between demineralization and sound tooth structure than visible reflectance and fluorescence without the interference of stains.[7–14]

The light scattering in sound enamel decreases as $1/\lambda^3$ with increasing wavelength from 400 to 1300 nm as shown in Fig. 1.[15] Enamel contains ~10% water, and water absorption increases beyond 1400 nm, also shown in Fig. 1. The Rayleigh-like wavelength dependence of the light scattering suggests that the scattering is mainly due to the individual enamel crystals that are much smaller than the wavelength of visible light.[15] Optical measurements at 1550 nm yielded a similar attenuation coefficient to that measured at 1310 nm; however, with an attenuation coefficient of only 2 to 3 cm^{-1}, it is extremely difficult to decouple the contributions of surface scattering and water absorption from the bulk scattering in the enamel.[16] The lesion contrast or contrast of demineralization arises due to the formation of pores in the enamel that highly scatter light. At 1300 nm, the scattering of the demineralized enamel increases by more than 2 orders of magnitude over sound enamel.[17]

Water may also play an important role in contributing to the lesion contrast. The water in sound enamel (~10% by volume) and in the underlying dentin (~22% by volume) can absorb incident photons.[1] At wavelengths beyond 1300 nm, most of the photons incident on the sound tooth penetrate through the transparent enamel to reach the highly scattering dentin. Therefore, higher water absorption likely reduces the intensity of light reflected from sound areas of the tooth.

Water can also fill the pores in the lesion markedly reducing the light scattering from the lesion. This phenomenon can be exploited to help differentiate active lesions from arrested lesions that have greatly reduced permeability.[18,19] Clinicians typically blow air over lesions for a few seconds during clinical examination to better view the lesion.

Recent studies suggest that there is reduced scattering at NIR wavelengths beyond 1600 nm for greater optical penetration in bone and soft tissues.[20,21] Standard InGaAs detectors are not sensitive past 1700 nm. New extended range InGaAs NIR cameras allow access to wavelengths beyond 1700 nm, and initial studies show higher contrast for lesions on occlusal surfaces from 1700 to 2350 nm; however, the sensitivity is not sufficient to use narrow-band filters to sample individual wavelengths, and the use of high intensity narrow-bandwidth diode-laser sources suffer from speckle interference.[22] In this letter, the teeth were scanned across the laser diode and fiber laser sources, and images were acquired using a single detector. Wavelengths of 1450, 1860, 1880, and 1950 nm were examined. The magnitude of water absorption is similar at 1450 and 1880 nm, whereas the magnitude of water absorption varies markedly between 1860,

*Address all correspondence to: Daniel Fried, E-mail: Daniel.Fried@ucsf.edu

1083-3668/2018/$25.00 © 2018 SPIE

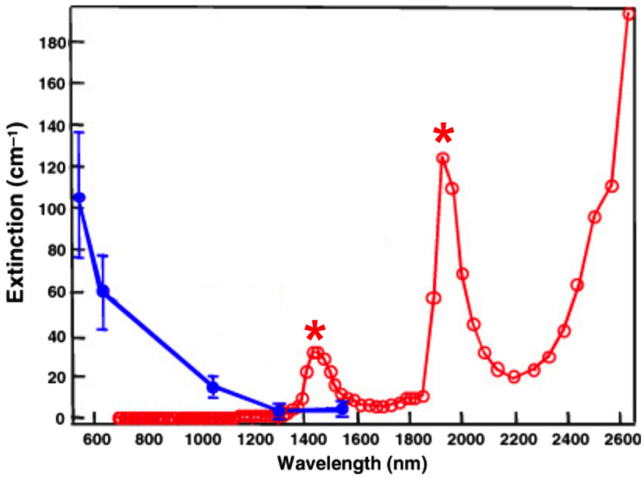

Fig. 1 Enamel attenuation spectra (blue) and water absorption spectra (red). Notable water absorption peaks are found at 1450 and 1940 nm (28.6 and 119 cm^{-1}, respectively).[14,15,24]

1880, and 1950 nm. Comparison of the contrast of early demineralization on tooth surfaces at these wavelengths allows us to estimate the contributions of reduced light scattering and water absorption at longer NIR wavelengths.

Ten human teeth with noncarious occlusal surfaces were collected and sterilized with gamma radiation. Tooth occlusal surfaces were abraded using air abrasion with 50-μm glass beads for 20 s to remove all stain and debris from the fissures and to remove the outermost fluoride-rich layers of enamel to facilitate the demineralization of those surfaces.[13] Next, teeth were mounted in black orthodontic acrylic blocks. Samples were stored in a moist environment of 0.1% thymol to maintain tissue hydration and prevent bacterial growth. The outlines of a 4×4 mm window (roughly 50-μm deep) were cut on the occlusal surfaces of each tooth using an Impact 2500 CO_2 laser from GSI Lumonics (Northville, Michigan) operating at a wavelength of 9.3 μm, pulse width of 15 μs, and repetition rate of 5 Hz. These markings served as a reference point to denote the demineralized area. The enamel surrounding the 4×4 mm windows was covered with acid-resistant varnish. Artificial lesions were created within the 4×4 mm windows by immersing each tooth into a 50-mL aliquot of a Ca/PO_4/acetate solution maintained at pH of 4.5 as described previously.[13] Varnish was removed using acetone after the lesions were generated [see Fig. 2(a)]. Using nondestructive cross-polarized optical coherence tomography (CP-OCT), we confirmed lesion presence and measured the lesion depth to be between 50- and 150-μm deep with intact surfaces [see Fig. 2(b)].[23–25]

Linearly polarized and collimated light from the NIR lasers was focused onto the tooth samples with an $f = 100$-mm lens. Computer-controlled XY motion control system ESP-301 and UTM150 stages from Newport (Irvine, California) were used to scan the samples for NIR reflectance image acquisition. Cross-polarized backscattered light from the tooth surface was collected with a model PDA10DT extended range InGaAs detector from Thorlabs (Newton, New Jersey). Laser light sources were: a 1468-nm superluminescent diode (SLD) with a bandwidth of 40 nm and a peak output of 14 mW, model 1480 from Exalos (Langhorne, Pennsylvania); a tunable

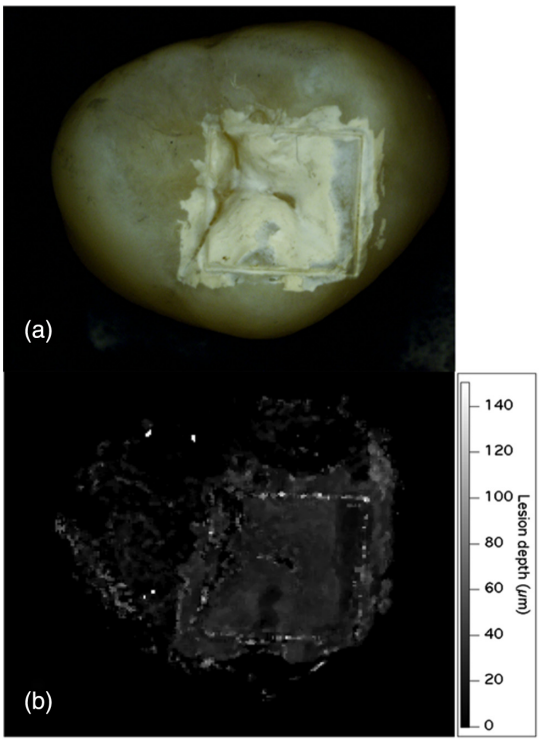

Fig. 2 (a) Digital microscopy image of one of the tooth samples with demineralization and (b) lesion depth map generated from CP-OCT scans.

1860- to 1880-nm thulium fiber laser with an output up to 2 W, model TLT-5 from IPG Photonics (Oxford, Massachusetts); and a linearly polarized 200-mW 1950-nm fiber laser, model AP-CW from AdValue Photonics (Tucson, Arizona). The 1468-nm source is not a narrow-bandwidth laser source, it is an SLD with a bandwidth of 40 nm, and water absorption varies from 28.6 cm^{-1} at 1448 nm to 19.8 cm^{-1} at 1488 nm with 25.6 cm^{-1} at 1468 nm.[26] The water absorption coefficients are 14.2, 31.1, and 113.5 cm^{-1} at 1860, 1880, and 1949 nm, respectively.[26]

These 10 samples were imaged with the point-to-point scanning system. Samples were air-dried for ~10 s prior to image acquisition. Each image was scanned with a highly reflective reference and normalized for comparison. The dot pitch between each scanned point was ~50 μm. The reflectance intensity was acquired and averaged over five iterations at each point.

For each sample and wavelength, the entire 4×4 mm window was summed and averaged to quantify the lesion intensity (I_L). A fixed 2×2 mm sound enamel area was selected outside the 4×4 mm window at each wavelength to calculate each sample/wavelength's mean sound intensity (I_S). Image contrast was calculated using $(I_L - I_S)/I_L$. The image contrast varies from 0 to 1 with 1 being very high contrast and 0 being no contrast/signal. Repeated measures analysis of variance followed by the Tukey–Kramer *post hoc* multiple comparison test was used to compare the image contrast at the four wavelengths. All quantitative analysis was done with IgorPro from Wavemetrics (Portland, Oregon) and Prism from Graphpad (San Diego, California).

Normalized point-to-point scanning reflectance images of two samples are shown in Fig. 3 for 1470, 1860, 1880, and 1950 nm. Demineralization appears whiter with higher intensity than sound enamel in these images. The higher reflectivity of the

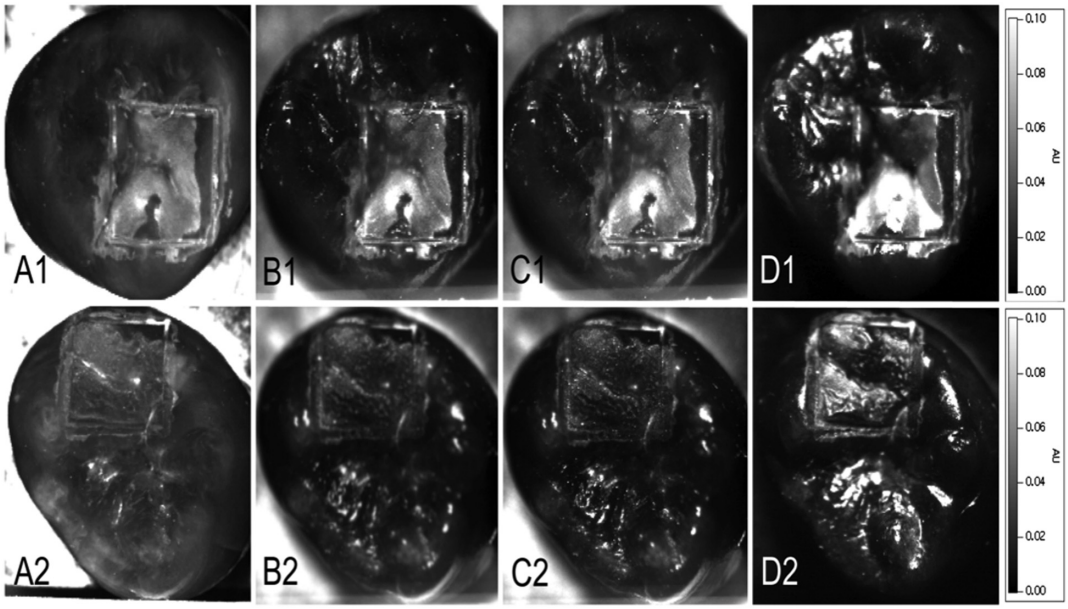

Fig. 3 NIR reflectance images generated by the point-to-point scanner for two tooth samples at (a1 and a2) 1470, (b1 and b2) 1860, (c1 and c2) 1880, and (d1 and d2) 1950 nm.

sound area outside the 4×4 mm windows is obviously higher for the shorter wavelength 1470-nm light even though the water absorption is as high as it is at 1860 nm. Sound enamel areas also appear darker at 1950 nm than at the other three wavelengths. The images appear similar although there are some differences in the images. Those differences are likely due to wavelength differences in the extinction of the polarizers and slight differences in the optical systems between the three laser systems. The lower extinction ratio of the polarizers is most obvious at 1950 nm where more specular reflection is clearly evident. The mean contrast $\pm$ standard deviation is plotted in Fig. 4 for the four wavelengths. The highest mean contrast was at 1950 nm—0.80 ± 0.07—and it was significantly higher ($p < 0.05$) than the other wavelengths. The contrast was similar at 1860 and 1880 nm, 0.68 ± 0.1 and 0.67 ± 0.09, respectively, and was significantly higher ($p < 0.05$) than at 1468 nm—0.33 ± 0.13.

A comparison of the lesion contrast for the four wavelengths suggests that the lesion contrast continues to increase beyond 1300 nm due to the decreasing scattering coefficient of enamel.

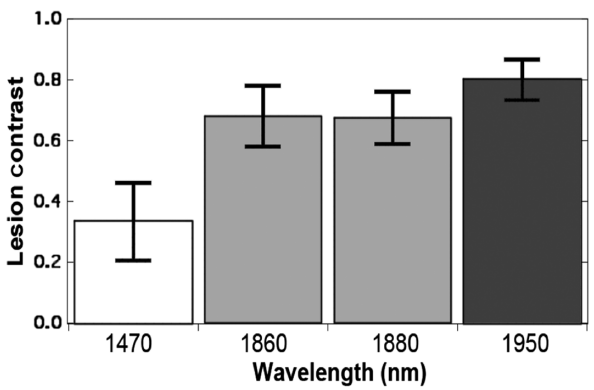

Fig. 4 Mean lesion contrast $\pm$ standard deviation ($n = 10$). Bars of the same color are statistically similar, $p > 0.05$.

There was no significant difference in the contrast between 1860 and 1880 nm even though the magnitude of water absorption at 1880 is more than twice as high as it is at 1860 nm. The contrast was much higher at 1880 compared to 1470 nm even though the magnitude of water absorption is similar. This observation was surprising to us, and we had suspected that water absorption contributed to a greater degree to the lesion contrast. However, this result does not contradict prior studies. In a previous study, we found that the lesion contrast was similar at 1450 and 1500 to 1750 nm.[12] The highest contrast was achieved at 1950 nm where the water absorption is eight times higher than at 1860 nm; however, the contrast was only slightly higher than at 1860 nm and that small increase in contrast can also be explained by the lower light scattering in the sound enamel.

There were some problems with the study, the most significant being the interference of specular reflection at 1950 nm and the use of three different laser systems. It is possible that specular reflectance may have influenced the contrast at 1950 nm; however, even without the 1950-nm data, it is obvious that light scattering in sound enamel continues to decrease with increasing wavelength beyond 1300 nm.

The most obvious implication of this study is the impact on the choice of wavelengths for caries detection and diagnosis. It appears that the use of longer wavelengths is advantageous for increasing the contrast of demineralization on tooth surfaces. In addition, these results suggest that it is not necessary to image at wavelengths coincident with the strong water absorption bands, such as 1450 or 1940 nm. The need for narrow-bandwidth sources poses additional challenges, including the difficulty of achieving sufficient intensity or throughput with low-cost broadband sources, such as tungsten–halogen lamps. In addition, the operation of optical coherence tomography (OCT) systems at wavelengths beyond 1300 nm has been proposed to achieve higher performance for imaging hard tissues.[7,8] This study provides the first evidence that light scattering in sound enamel significantly decreases beyond 1300 nm, which may be advantageous for achieving greater imaging depths for OCT.

Disclosures

The authors declare they have no competing financial interests.

Acknowledgments

This work was supported by the National Institutes of Health/ National Institute of Dental and Craniofacial Research Grant Nos. R01-DE01963, R01-DE14698, and F31-DE026350. We would like to thank Nathaniel Fried for loan of the IPG photonics laser.

References

1. O. Fejerskov and E. Kidd, Eds., *Dental Caries: The Disease and Its Clinical Management*, Blackwell, Oxford (2003).
2. G. K. Stookey, "Quantitative light fluorescence: a technology for early monitoring of the caries process," *Dent. Clin. North Am.* **49**(4), 753–770 (2005).
3. S. Tranaeus et al., "In vivo repeatability and reproducibility of the quantitative light-induced fluorescence method," *Caries Res.* **36**(1), 3–9 (2002).
4. R. R. Alfano et al., "Human teeth with and without caries studied by laser scattering, fluorescence and absorption spectroscopy," *IEEE J. Quantum Electron.* **20** 1512–1516 (1984).
5. A. F. Ferreira Zandona et al., "An in vitro comparison between laser fluorescence and visual examination for detection of demineralization in occlusal pits and fissures," *Caries Res.* **32**(3), 210–218 (1998).
6. A. F. Zandona and E. Epure, "Evolution of caries diagnosis," *Decisions Dent.* **4**(2) 43–46 (2018).
7. R. S. Jones et al., "Near-IR transillumination at 1310-nm for the imaging of early dental caries," *Opt. Express* **11**(18), 2259–2265 (2003).
8. C. Buhler, P. Ngaotheppitak, and D. Fried, "Imaging of occlusal dental caries (decay) with near-IR light at 1310-nm," *Opt. Express* **13**(2), 573–582 (2005).
9. J. Wu and D. Fried, "High contrast near-infrared polarized reflectance images of demineralization on tooth buccal and occlusal surfaces at $\lambda = 1310$-nm," *Lasers Surg. Med.* **41**(3), 208–213 (2009).
10. C. Zakian, I. Pretty, and R. Ellwood, "Near-infrared hyperspectral imaging of teeth for dental caries detection," *J. Biomed. Opt.* **14**(6), 064047 (2009).
11. M. Staninec et al., "In vivo near-IR imaging of approximal dental decay at 1,310 nm," *Lasers Surg. Med.* **42**(4), 292–298 (2010).
12. S. Chung et al., "Multispectral near-IR reflectance and transillumination imaging of teeth," *Biomed. Opt. Express* **2**(10), 2804–2814 (2011).
13. W. A. Fried et al., "High contrast reflectance imaging of simulated lesions on tooth occlusal surfaces at near-IR wavelengths," *Lasers Surg. Med.* **45**(8), 533–541 (2013).
14. J. C. Simon et al., "Near-IR transillumination and reflectance imaging at 1300-nm and 1500-1700-nm for in vivo caries detection," *Lasers Surg. Med.* **48**(6), 828–836 (2016).
15. D. Fried et al., "Nature of light scattering in dental enamel and dentin at visible and near-infrared wavelengths," *Appl. Opt.* **34**(7), 1278–1285 (1995).
16. R. S. Jones and D. Fried, "Attenuation of 1310-nm and 1550-nm laser light through sound dental enamel," *Proc. SPIE* **4610**, 187–190 (2002).
17. C. L. Darling, G. D. Huynh, and D. Fried, "Light scattering properties of natural and artificially demineralized dental enamel at 1310-nm," *J. Biomed. Opt.* **11**(3), 034023 (2006).
18. R. C. Lee, C. L. Darling, and D. Fried, "Activity assessment of root caries lesions with thermal and near-infrared imaging methods," *J. Biophotonics* **10**(3), 433–445 (2016).
19. R. C. Lee et al., "Infrared methods for assessment of the activity of natural enamel caries lesions," *IEEE J. Sel. Top. Quantum Electron.* **22**(3), 6803609 (2014).
20. L. A. Sordillo et al., "Deep optical imaging of tissue using the second and third near-infrared spectral windows," *J. Biomed. Opt.* **19**(5), 056004 (2014).
21. J. R. Weber et al., "Towards a bimodal proximity sensor for in situ neurovascular bundle detection during dental implant surgery," *Biomed. Opt. Express* **5**(1), 16–30 (2013).
22. C. Ng et al., "SWIR reflectance imaging of demineralization on the occlusal surfaces of teeth beyond 1700-nm," *Proc. SPIE* **10473**, 104730U (2018).
23. R. S. Jones et al., "Imaging artificial caries on the occlusal surfaces with polarization-sensitive optical coherence tomography," *Caries Res.* **40**(2), 81–89 (2006).
24. H. Kang et al., "Nondestructive assessment of early tooth demineralization using cross-polarization optical coherence tomography," *IEEE J. Sel. Top. Quantum Electron.* **16**(4), 870–876 (2010).
25. K. H. Chan et al., "Use of 2D images of depth and integrated reflectivity to represent the severity of demineralization in cross-polarization optical coherence tomography," *J. Biophotonics* **8**(1–2), 36–45 (2015).
26. G. M. Hale and M. R. Querry, "Optical constants of water in the 200-nm to 200-μm wavelength region," *Appl. Opt.* **12**, 555–563 (1973).